Cleaner Engineering and Technology 32 (2026) 101218

Contents lists available at ScienceDirect

Cleaner Engineering and Technology

journal homepage: www.sciencedirect.com/journal/cleaner-engineering-and-technology

Circular insulation material: characterisation and bio-solubility of waste mineral wool for blown-in insulation applications

S. Tumkur Karnick *, N. Lushnikova, F. Gauvin, H.J.H. Brouwers

Department of Built Environment, Eindhoven University of Technology, P. O. Box 513, Eindhoven, 5600 MB, the Netherlands

ARTICLE INFO

Keywords:
Mineral wool
Mechanical recycling
Circular building materials
Insulation material
Bio-solubility

ABSTRACT

Mineral wool is extensively utilized worldwide for thermal and acoustic insulation in buildings. However, the widespread use of these materials has led to a significant increase in construction and demolition (C&D) waste, much of which is either landfilled or incinerated. With the increasing emphasis on sustainability and circular economy practices, the low-energy recycling of mineral wool waste as blown-in insulation emerged as a promising pathway to reduce landfill burdens, conserve resources, and close material loops with minimal processing. This study aims to investigate the chemical and physical properties of the shredded waste mineral wool as well as its health and safety aspects in order to be reused as a blown-in insulation. To benchmark performance and safety of short fibers, a comparative analysis was also conducted against virgin mineral wool samples. The waste mineral wool insulation boards were shredded into loose form, which were then characterized using chemical methods such as FTIR and XRF. The physical properties such as bulk density, thermal conductivity, water absorption, vapour sorption and water contact angle were also analyzed. In addition, an in-vitro dissolution test was conducted to assess the bio-solubility of short inorganic fibres. Despite having a lower silicon content, XRF revealed that the chemical compositions of waste mineral wool were similar to virgin counterparts. Although the thermal conductivity of waste mineral wool increases, the λ-value remained within the permissible range, indicating its potential use in blown-in insulation. The in-vitro bio-solubility of short fibres through a batch dissolution method showed that all the samples except waste stone wool reached the threshold level after 14 days.

1. Introduction

The demand for mineral wool is escalating due to demanding energy efficiency standards in the construction sector. The global mineral wool market is USD 733.45 million in 2024, with expectations to reach USD 776.73 million in 2025 and USD 1188.55 million by 2033. Europe, with 35% of the worldwide industry dominates this market driven by strict building regulations and EU energy efficiency initiatives that encourage sustainable construction (Mineral Wool Insulation Material Market, 2024). The European construction sector is undergoing a significant transformation as it becomes imperative to decouple economic growth from resource use and carbon emissions. Buildings consume more than 40% of the total energy in the European Union and 50% of the region's gas supply. Approximately 80% of this energy is utilized for heating (Directive (EU), 2024). In 2022, glass wool (GW) and stone wool (SW) contributed to 33% and 23%, respectively, of Europe's thermal insulation market, whereas the renewable insulation material was 2% (Consultants, 2023). SW is anticipated to last at least 75 years in buildings; it is still a sought-after insulation material despite its environmentally demanding production method (Straub et al., 2011).

Unfortunately, after 20 years, a lot of waste mineral wool ends up in mixed containers for landfilling or incineration because of roof cover deterioration or demolition (Acar et al., 2024). As a result, the amount of mineral wool waste produced each year keeps rising (Väntsi and Kärki, 2014) and the total amount of mineral wool waste generated in the EU is expected to grow up to 2.82 million tons by 2030 (Yap et al., 2021). Most of this waste is landfilled, a practice that is problematic due to its low bulk density (8–100 kg/m^3) and poor compressibility (Sattler et al., 2020).

In recent years, the circular economy (CE) framework has drawn a lot of attention because it views waste valorization, controlling finite stocks with balanced flows of renewable resources, and reducing reliance on primary resources as ways to separate economic growth from environmental degradation (Rahla et al., 2021; Komkova et al., 2025). Due to

* Corresponding author.
E-mail address: s.tumkur.karnick@tue.nl (S.T. Karnick).

https://doi.org/10.1016/j.clet.2026.101218
Received 17 October 2025; Received in revised form 25 March 2026; Accepted 21 April 2026
Available online 21 April 2026

high prices, lack of supply chains, and technological challenges, mineral wool recycling in a closed-loop circular economy is still in its early stage (Väntsi and Kärki, 2014; Sattler et al., 2020; Superti et al., 2021). The EU CE action plan emphasizes the reduction of waste and the high-value recycling of construction materials, while the renovation wave promotes material efficiency and sustainable insulation in large scale building renovations. The Revised Construction Products Regulation (EU) 2024/3110 and the Ecodesign for Sustainable Products Regulation (ESPR) (EU) 2024/1781 implement digital product passports and enhance sustainability reporting, promoting reuse and recycled materials. In conjunction with the Level(s) framework for comprehensive life performance, these tools establish a distinct demand for circular insulating solutions, such as mechanically recycled mineral wool, hence minimizing landfill and primary resource consumption (A New Circular Economy Action, 2024; Regulation - EU - 2024/3110 - EN - EUR-Lex, 2024; Regulation (EU) 2024/1781 - EN - EUR-Lex, 2024; Level(s)).

A recent study has shown the possibility of direct reuse of old insulation panels (Acar et al., 2024) as a secondary insulation material. Also, several research have been done to upcycle mineral wool from construction and demolition (C&D) waste as a component of alkali-activated materials (Koh et al., 2024; Pavlin et al., 2021), as a secondary raw material for aerogel manufacturing (Borzova et al., 2025), and as supplementary cementitious materials (Doschek-Held et al., 2024), multifunctional materials (Zhong et al., 2025a), magnetic oil absorbents (Zhong et al., 2025b).

Despite these recent innovations, upcycling of waste mineral wool and conventional recycling through remelting remain complex, energy-intensive and are hindered by contamination and material heterogeneity (Väntsi and Kärki, 2014; Yliniemi et al., 2018; EURIMA). Usually, complex processes result in higher costs, which is contrary to the goal of waste treatment. However, Domonkos et al., demonstrated the less energy-intensive recycling using a micro-mill and gear crusher to recycle old insulation panels into short fibers. These short fibres can then be used with or without treatment as blown-in or loose-fill insulation in open attics and ceilings, or as filling insulation in hollow constructions, such as cavity walls (Domonkos et al., 2022).

Furthermore, health and safety considerations for individuals interacting with the short fibres during handling or installation, are a significant requirement. Although the chemical composition of mineral wool was changed in the 1990s to increase the bio-solubility and reduce carcinogenic risk (Christensen et al., 1994), concern persists regarding respirable fibers. According to the World Health Organization (WHO), fibres having a length greater than 5 μm, a diameter less than 3 μm as well as an aspect ratio greater than 3, are the criteria for 'respirable fibers' and may penetrate the alveolar region of the lungs (WHO, 1997). Fibres above 20 μm evade macrophage clearance and may induce lung damage due to their bio-persistence (Health Effects Institute-Asbestos Research, 1991).

In this regard, Cannizzaro et al., have studied the *in-vitro* dissolution behaviour of four high-temperature insulation wools in simulating physiological fluid (Cannizzaro et al., 2019). On the other hand, Guldberg et al., have presented both *in-vivo* and *in-vitro* studies on various industrially available glass and stone wool fibers and correlated dissolution mechanisms with chemical composition (Guldberg et al., 1998, 2000, 2002). Wohlleben et al., investigated the bio-solubility of stone wool samples sourced from various construction sites and producers (Wohlleben et al., 2017). Additionally, the effect of different synthetic lung fluids and binder content on the dissolution have also been studied in the recent past (Sauer et al., 2021; Barly et al., 2019). All these previous studies provide a thorough understanding of the effect of chemical composition, binder content, type of lung fluid and dissolution methods on mineral wool's bio-solubility, but none of these studies were conducted on waste mineral wool samples except Wohlleben et al.

Therefore, the current study aims to exhibit a simple circular strategy of recycling waste mineral wool and to evaluate whether waste mineral wool retains the critical properties necessary for building insulation, especially for blown-in insulation. This includes a comprehensive characterization of the chemical, physical and bio-solubility properties of shredded waste mineral wool and comparing them with those of virgin mineral wool. Fig. 1 shows the necessary steps included in this research.

2. Materials and methods

2.1. Materials

The waste glass wool (WGW) and waste stone wool (WSW) insulation panels were obtained and processed by Kruiswijk Groep B.V. from old office buildings that were built in the 1970s and insulated in 1995 in Gouda, the Netherlands. The waste glass wool had previously been employed as an insulation material in the ceilings and walls of the building, while the waste stone wool was utilized for fire separation in these facilities. Virgin blown-in insulating materials – virgin glass wool (VGW) for cavity walls and virgin stone wool (VSW) were used as reference samples for comparative tests. Waste of mineral wool insulation boards was mechanically treated in the rotating shredding mill (Lidem, MT15V2) by Takkenkamp Groep B.V, which provides chopping and crushing sizes between 5 and 50 mm. All the samples in the loose form are shown in Fig. 2.

For the bio-solubility test, a modified gamble solution (HCl; Rockwool) was prepared using ACS purity grade salts and deionized water. The following salts were provided by Thermo-Fischer, Magnesium chloride hexahydrate ($MgCl_2.6H_2O$, 99+ %), Sodium chloride (NaCl, 99 %), Calcium chloride dihydrate ($CaCl_2.2H_2O$, 99+ %), Sodium sulphate (Na_2SO_4, 99 %), Sodium phosphate dibasic heptahydrate ($Na_2HPO_4.7H_2O$, 98+ %), Sodium Bicarbonate ($NaHCO_3$, 99.7+ %), Sodium Tartrate Dihydrate (Na_2-tartrate.$2H_2O$, 99-101%), Sodium citrate dihydrate (Na_3-citrate.$2H_2O$, >99 %), 90 % lactic acid, Glycine ($C_2H_5NO_2$, >99 %), Sodium pyruvate ($C_3H_3NaO_3$, 99%). HCl and formaldehyde were used in the preparation of the modified gamble solution.

2.2. Methods

2.2.1. Chemical characterisation

Fourier Transform Infrared Spectroscopy (FTIR): Using the Frontier Spectrometer from PerkinElmer, Fourier transform infrared spectroscopy was conducted in the range of 400 cm^{-1} to 4000 cm^{-1} with 20 scans per measurement. This technique was employed to characterise the functional groups present in the mineral wool samples.

X-ray fluorescence (XRF): Initially, loss-on-ignition was carried out for 4 h on the virgin glass wool and waste glass wool at 550 °C to avoid melting and on the virgin stone wool and waste stone wool at 850 °C. Subsequently, the solid mineral wool samples were mixed with a 67% $Li_2B_4O_7$-33% $LiBO_2$ anhydrous fusion mixture in a 1:10 ratio, and 170 μl of 2 M LiBr was added to create the fused beads. The chemical composition of these fused samples was then analyzed using X-ray fluorescence on a PANalytical instrument.

2.2.2. Physical characterisation

Bulk density: Bulk density in a loose state was determined by weighing the sample in the mould of a known volume. The mean value of the three tests was considered representative. For the determination of bulk density under a specific load, a modified procedure from IS 3144:1992 was used. The steel loads press a known volume of wool that is initially placed inside the mould in a loose state. A load of 0.2, 0.4, 0.7 and up to 10 kg may be added, and the reduction of height of the compressed wool is measured. The test stops as there is no reduction in the height of the sample. The bulk density in the compressed state is the mass of a material divided by its volume after compaction. An average value of three samples was considered.

Moisture content, water vapour sorption, water absorption, and

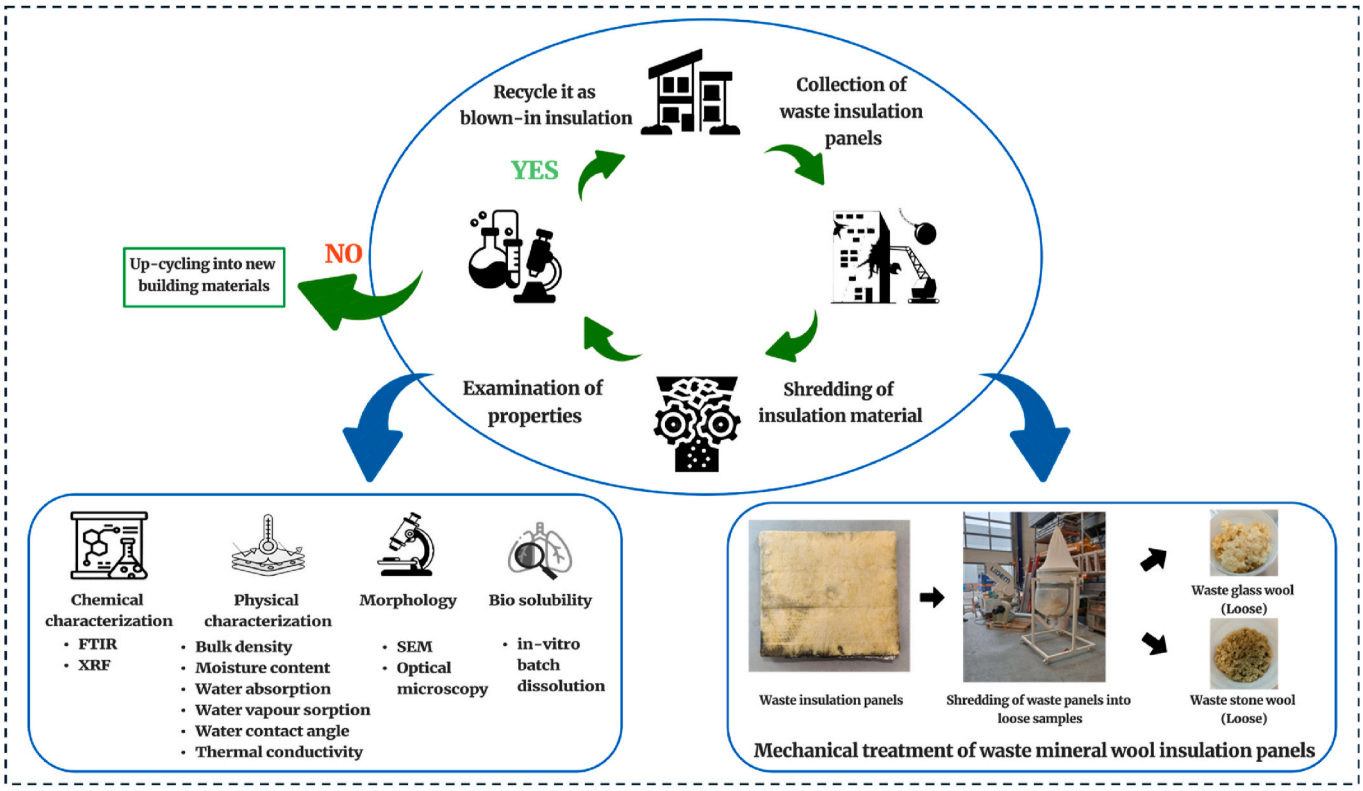

Fig. 1. Schematic representation of recycling mineral wool waste into blown-in insulation.

Fig. 2. Samples of mineral wool in loose form.

water contact angle

The moisture content of the samples was measured by drying in the oven at 60 °C of the samples of mineral wool for 24 h. The moisture content was calculated as follows:

$$W_A = \frac{m_2 - m_1}{m_2} \times 100 \quad (1)$$

where m_1 – weight of the dry sample (g), m_2 – weight of the wet sample (g).

Water vapour sorption of all the mineral wool samples was evaluated according to the ASTM C1104/C 1104 M-00 standard. The test was conducted at a temperature of 50 °C and a relative humidity of 95 ± 3 % for a duration of 96 h. The samples were placed inside a container with water at the bottom to maintain the desired humidity. To ensure uniform relative humidity, a humidity sensor and a fan were installed at the top of the container, which was then placed within a climate chamber set to 50 °C. The experimental setup is illustrated in Fig. 3. Later, these samples were used for thermal conductivity measurement as wet samples. The mean value of three samples was considered.

Water absorption was tested according to the modified loose wool sample procedure from EN 12087. The dry samples of wool, preliminary weighed (m_0), had been saturated with water at (24 ± 0.5) h at (23 ± 5) °C. Then the samples were placed on a mesh to drain the water for (10 ± 0.5) min. Then the sample was weighed to assess m_{24}. An average value of three samples was considered.

The water absorption by weight was calculated as:

$$W_A = \frac{m_{24} - m_0}{m_0} \times 100 \quad (2)$$

where m_0 – mass of the sample in dry state (g), m_{24} – mass of the sample in saturated state (g).

Water contact angle was measured for all four samples using the Dataphysics Contact Angle System to assess their hydrophobicity. The samples were spread uniformly on a glass slide coated with double-sided tape, and a 10 μl water droplet from Milli-Q was placed on each sample

Fig. 3. Experimental setup of water vapour sorption test; (a) water bath at the bottom; (b) samples above the water bath; (c) humidity sensor and a fan setup; (d) climate chamber.

to determine the contact angle.

Thermal conductivity: Thermal conductivity measurements were acquired using the Hot Disc Thermal Constants Analyzer (TPS 2500 S) at an ambient temperature of 21 °C. Mineral wool samples which were dried at 50 °C were considered as dry samples and vapour adsorbed samples were considered as wet samples. Individual tests were carried out on these samples by placing them in two 3D printed molds (50 × 50 × 50 mm), and each mould was wrapped with a polyethylene film. A polyethylene film was used due to its good particle packing and low thickness, which won't interfere with the results. 7577F1 sensor was placed in the middle of these molds. The measurement duration was 10 s at 5 m W. It was performed five times, and the average was recorded as the result with the lowest achievable standard deviation (less than 1 m K).

2.2.3. Morphology characterization

Scanning electron microscopy (SEM): Morphological and chemical changes of the fibres before the treatment and after the leaching and dissolution process were investigated using SEM (Phenom ProX, ThermoFischer) at an acceleration voltage of 10 kV. Both secondary electron detectors and back scattering were employed to characterise the fiber surface following dissolution. Before the examination, all the samples were sputter-coated with gold for 30 s and 30 mA.

Optical microscopy (OM): Dimensional analysis, such as lengths (L), diameters (D) and aspect ratio (L/D), was measured for 250 fibres of each sample before bio-solubility test using optical microscopy (Zeiss Axiocam 305). The mineral wool samples were initially dispersed in isopropanol and subsequently placed between the glass plates.

2.2.4. Bio-solubility test (static batch dissolution)

Modified gamble (MG) solution: A modified gamble (MG) solution (HCl; Rockwool) with HCl as a buffer was prepared by the methodology described by Guldberg et al. (1998). This MG solution was selected due to its composition, which aligns with the EURIMA guidelines (EURIMA and European Parliament and Council, 2008).

The composition of the MG solution utilized in this research is detailed in Table 1. Organic and inorganic components were initially prepared separately in 500 mL High-Density Polyethylene (HDPE) bottles and subsequently combined into a single solution. Hydrochloric acid was employed as a buffer to maintain the pH at 4.5, and 2 mL of formaldehyde was added to inhibit mould growth.

Bio-solubility test: The batch dissolution method was employed at a temperature of 37 ± 1 °C without stirring but with periodic shaking. Dissolution was assessed at intervals of 1, 3 h, and 1, 3, 7, 14, 21, and 28 days. For each time interval, a separate sample was prepared. For the samples at 7, 14, 21, and 28 days, a one-time HCl recharge was performed by adding a few drops to maintain the pH at 4.5. Solutions were filtered using 0.22 μm filters, and the pH was measured immediately post-filtration.

Table 1
The composition of the modified gamble solution (Guldberg et al., 1998).

Chemical	Concentration (g/L)
$MgCl_2{\cdot}6H_2O$	0.212
NaCl	7.12
$CaCl_2{\cdot}2H_2O$	0.029
Na_2SO_4	0.079
$Na_2HPO_4{\cdot}7H_2O$[a]	0.28
$NaHCO_3$	1.95
Na_2-tartrate$\cdot 2H_2O$	0.18
Na_3-citrate$\cdot 2H_2O$	0.152
90% lactic acid	0.14
Glycine	0.118
Na-pyruvate	0.172
HCl	1000
formaldehyde	2 (mL/L)

[a] Substitute of Na_2HPO_4. Calculations are done accordingly.

Inductively coupled plasma-optical emission spectrometry (ICP-OES): Aliquots (30 mL) of the test solution from each sample were transferred to plastic containers for elemental concentration analysis via ICP-OES (Spectroblue FMX36 from Spectro). For quantification, external multi-standards were utilized. Certified reference materials, including Multistandard IV (1.11355), Multistandard XVI (1.09487), and Si standard (1.70365) from Certipur, were employed. Standard IV was used for calibration when elements were present in both multi-standards. The tested fibres were subsequently dried at 50 °C in an oven for one day and analyzed using Scanning Electron Microscopy (SEM).

3. Results and discussion

3.1. Chemical characterisation

3.1.1. FTIR

Functional groups O-H, C-H, and C=O are present in the waste glass wool samples, according to the spectra in Fig. 4. Water that has been adsorbed onto the glass wool during its consumption as an insulation material in the buildings is represented by the band at 3777 cm^{-1} (Criado et al., 2014). WGW, WSW, and VSW all have peaks at about 2900 cm^{-1}, which are indicative of an aliphatic C-H bond present in an organic binder (Asemani and Rabbani, 2020), (Coury and Dillner, 2008). However, VGW samples lack organic binders, so this peak is absent. Furthermore, the stretching vibration of C=O, which is found in

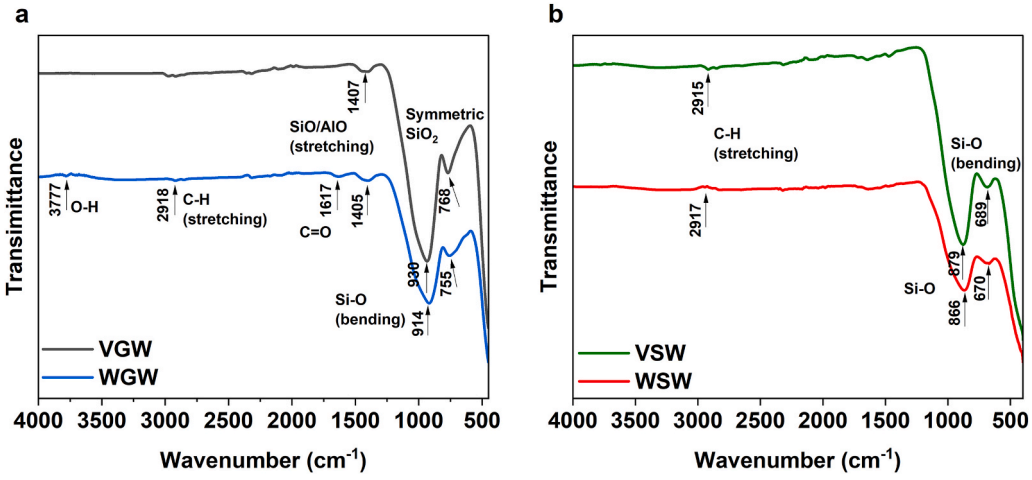

Fig. 4. FTIR spectra of (a) glass wool samples; (b) stone wool samples.

organic binders in the form of aldehydes or carboxyl groups, is shown by the peak at 1617 cm^{-1} for WGW (Lin et al., 2019). Phenol-urea-formaldehyde (PUF) is the most common type of organic binder used in mineral wool (Rywotycki et al., 2024), and also based on the data of Yliniemi et al. (2021), it was assumed that waste mineral wool used in this research contained PUF binder. Additionally, in glass wool samples, the spectrum exhibits a significant band at approximately 1400 cm^{-1}, which is attributed to the SiO/AlO stretching vibration. Also, characteristics of silica material, the bending and symmetric modes of SiO_2 are found in all the samples at 920 and 755 cm^{-1}, respectively (Dastorian Jamnani et al., 2016). Therefore, these findings highlight the major differences in the chemical compounds present in the waste mineral wool during its lifecycle and illustrates that determining the composition and contaminants is crucial for the establishment of the Digital Product Passport in accordance with ESPR (Regulation (EU) 2024/1781 - EN - EUR-Lex, 2024).

3.1.2. XRF

According to Table 2 the main elemental oxides present in VGW samples are 57.10% SiO_2, 30.87% Na_2O, 2.55% MgO, and 7.95% CaO, which was a similar composition to soda lime silicate glass (Martin, 2006). WGW possessed a comparable composition; however, it contained slightly less SiO_2, perhaps due to variations in the raw materials utilized. Additionally, WGW samples contained 0.2% Fe_2O_3, which exceeded the normal concentration of <0.1% (Guldberg et al., 2000). Although the XRF method employed in this study cannot identify boron, investigations in the literature indicated that glass wool contains 4–11 wt% B_2O_3 (Yliniemi et al., 2021). The loss-on-ignition (LOI) at 550 °C for WGW showed the presence of organic content of approximately 6-8%, however, the VGW had a mere 0.28% of organic content, which might be some dust particles. Usually, to improve the finished products' stiffness and make the compaction process easier, 5–10 wt % of organic binders are often added during the mineral wool production (Yliniemi et al., 2018). In addition, waste mineral wool samples contain other contaminants such as mycological substances, dust particles or other chemical substances, which can be seen in Fig. 1. Yap et al., also mentioned the presence of such contaminants in their work (Yap et al., 2021).

Similarly, Table 2 indicates that VSW and WSW possess analogous compositions, with SiO_2, Al_2O_3, CaO, and Fe_2O_3 as the predominant minerals. This verified their basaltic composition (Agency for Toxic Substances and Disease Registry (US), 2004). Also, LOI was conducted at 850 °C on VSW and WSW samples, and the results showed the presence of organic binders, which were 2.52% and 3.12%, respectively.

All samples exhibited trace levels of heavy metals, including Cr_2O_3, CuO, and ZnO in glass wool, and V_2O_5, Cr_2O_3, CuO, NiO, and ZnO in stone wool. These elements exist at low concentrations and are confined within the glassy matrix, presenting no immediate environmental hazard during reuse. Leaching may occur under strongly acidic (Nilsen et al., 2003) or alkaline (Snellings, 2013) environments. Given the constraints of XRF in identifying trace components without calibration standards, these findings ought to be analyzed qualitatively rather than quantitatively (Ramsey et al., 1995).

XRF study indicates that both waste and virgin mineral wool possess comparable major oxide compositions. Elevated LOI values in waste samples signify the presence of residual organic binders and contaminants, although trace heavy metals do not provide a substantial danger for reuse in blown-in insulation applications.

3.2. Physical characterisation

3.2.1. Bulk density

Bulk density is one of the critical parameters needed to assess the thermal conductivity of an insulation material. As shown in Table 3, the

Table 3
Bulk density in different load conditions.

Sample	Bulk density (kg/m^3)	
	Loose state	Compressed state
VGW	38.7 ± 0.39	41.3 ± 0.37
WGW	36.9 ± 0.08	39.2 ± 0.16
VSW	63.9 ± 3.33	68.0 ± 3.63
WSW	70.6 ± 3.00	75.2 ± 2.84

Table 2
X-ray fluorescence oxide composition of different mineral wool samples.

Composition	Na_2O	MgO	Al_2O_3	SiO_2	K_2O	CaO	TiO_2	Fe_2O_3	Other	LOI
VGW	30.87	2.55	0.85	57.10	0.19	7.95	0.02	0.11	0.40	0.28
WGW	27.95	2.51	2.90	49.94	0.95	6.07	0.13	0.19	2.33	8.30
VSW	0	9.39	18.89	40.67	0.78	17.58	1.48	7.85	0.82	2.52
WSW	0	10.66	18.34	39.97	1.11	16.53	2.35	7.27	0.62	3.12

bulk density of VGW was slightly higher than WGW by around 4% and 5% in both loose and compressed states, respectively. However, the value of bulk density for WSW increased by 10% in both loose and compressed states compared to its virgin counterpart. The increase in the bulk density for stone wool samples could be related to its fiber density, which is also higher than the glass wool samples. In addition, the bulk density became constant after the application of load reached 10 N for glass wool samples and 17 N for stone wool samples.

3.2.2. Moisture content, water vapour sorption, water absorption, and water contact angle

After the loss-on-drying, the inherent moisture content values were found to be around 0.4% for all the samples. Water absorption tests (Table 4) revealed that VGW and VSW absorbed less moisture than their waste counterparts. WSW demonstrated a remarkable 101% increase compared to VSW's water absorption, while WGW showed a 33% higher water absorption than VGW. WGW had a higher water affinity than WSW among waste samples.

Similar trends were seen in vapour adsorption, where WGW adsorbs about 37% more moisture than VGW, whereas vapour sorption in WSW and VSW were almost 4-5 times lower compared to glass wool samples.

The increased moisture sensitivity of waste samples is ascribed to aging effects, encompassing the deterioration of phenol-formaldehyde binders and alterations in fiber structure. Environmental circumstances could promote binder hydrolysis because phenolic hydroxyl and hydroxymethyl groups make it easier for moisture to get in and make the resin structure weaker. (Kläusler et al., 2013; Yu et al., 2018). The other reason would be the accessibility of open voids within old glass wool samples that allows water to readily displace air which increases the water absorption (Doggett, 2020; Rengasamy, 2006). Additionally, measurements of the water contact angle (Fig. 5) verified that waste mineral wool was less hydrophobic than virgin samples, especially WGW.

3.2.3. Thermal conductivity

Thermal conductivity for all the samples in different conditions (dry, wet (after water vapour sorption), loose and compressed) are shown in Table 5. The amount of moisture content in the wet samples can be seen in Table 4.

The primary factor influencing the thermal conductivity (λ) of dry mineral wool was its bulk density. In wet conditions, it was contingent upon both density and moisture content. The bulk densities of loose samples ranged from 40 to 70 kg/m^3, while the bulk densities of compressed samples ranged from 70 to 150 kg/m^3. The lighter materials, such as glass wool in dry conditions, contained lower amounts of fibres per unit volume with more air voids compared to the denser materials like stone wool.

As seen from Fig. 6a, the VGW had the lowest thermal conductivity in dry and loose conditions when the corresponding bulk density reached 38.09 kg/m^3. For an increased bulk density of 83.01 kg/m^3 in the compressed state, the λ-value of dry VGW increased by a marginal 5% compared to its counterpart in the loose state. As evident from the results, the λ-value of the virgin materials remained stable even when their bulk density was altered. The dry WGW sample at a bulk density of 42.33 kg/m^3 exhibited an increase in its thermal conductivity (loose state) by 19% compared to the VGW sample under the same condition. Similarly, an increase of 15% was observed in dry and compressed WGW compared to VGW. The thermal conductivity of the loose WSW in dry conditions was marginally higher (2%) than the VSW in the same conditions.

The λ-value of WSW exhibited an upward trend, increasing by 14% (compressed and dry) and 38% (compressed and wet) relative to VSW under comparable conditions, attributable to the rise in bulk density and moisture content. Conversely, VSW's thermal conductivity had an inverse relationship with its bulk density. VSW with elevated bulk density and moisture content demonstrated superior thermal conductivity compared to those with reduced bulk density, resulting in a 15% decrease in λ-value. A comparable tendency was noted with loose WGW samples in wet conditions, where it exhibited superior performance relative to VGW in analogous circumstances. Jiřičková et al., demonstrated similar results for wet insulation materials. Consequently, the water in the material is primarily present as droplets that are dispersed very randomly. Due to hydrophobization in case of WGW, water cannot directly contact the fibres, and even mineral wool with no surface treatment has very low wettability (Jiřičková et al., 2006). Although dry VSW at different bulk densities shows the same trend, the marginal change was within the range (Jiřičková et al., 2006).

Usually, the range for thermal conductivity of dry glass and stone wool will be between 0.023 and 0.040 W/m·K and 0.033 to 0.046 W/m·K, respectively (Glass Wool; Hasanzadeh et al., 2023). Abi-Jdayil et al., have also mentioned that the thermal conductivity of mineral wools rose from 0.037 W/m·K to 0.055 W/m·K with a mere 10 vol% increase in moisture content (Abu-Jdayil et al., 2019). Furthermore, the λ-values of the waste mineral wool materials investigated in this research were compared to the available data in the existing literature, and the results are summarized in Table 6. Therefore, λ-values of both WGW and WSW are within the acceptable range as mentioned above, and are suitable for the lifecycle extension in the form of blown-in insulation.

Table 4
Water absorption and vapour sorption.

Sample	Water absorption (%)	Water vapour sorption (%)
VGW	634 ± 0.81	14.44 ± 3.02
VSW	281 ± 0.46	3.66 ± 1.85
WGW	839 ± 0.84	19.76 ± 8.96
WSW	565 ± 0.40	4.20 ± 2.11

3.3. Morphology characterization

3.3.1. SEM

The microstructure and morphology characterisation of all the mineral wool samples was done before and after conditioning them over different time periods. Fig. 7 shows the SEM scans of the mineral wool samples before the bio-solubility test, which indicates the absence of surface erosion and other deformations except organic binder material in VSW, WGW and WSW.

After the bio-solubility test, SEM scans (Fig. 8) showed that the morphology of all the mineral wool samples changed due to the surface erosion and the formation of Si-rich gel layers that prevent further dissolution. A study by Wohlleben et al. have shown the correlation between the presence of organic binders and the tendency to form gels (Wohlleben et al., 2017) and validate the results of this study.

All the samples containing the organic binders such as WGW, WSW and VSW demonstrated the characteristic gel formation (c), formation of bubbles (e) and collapse of bubbles (f). This type of amorphous gel formation further hindered the dissolution of the mineral wool, due to the solution becoming supersaturated. However, such structures were not observed in the case of VGW, due to the absence of organic binders. As seen in WGW (1st row), the highest degradation takes place between 7 and 21 days, which can be correlated with ICP results for Si dissolution (Fig. 9). Similar degradation occurred with WSW around the same time, with noticeable collapsed bubbles (f) and leaching pits (d) (2nd row). However, in VSW, collapsed bubbles and leaching pits were not observed (4th row). Despite having organic binders, waste mineral wool disintegrated predominantly in terms of microstructural analysis compared to those without binders. Although the dissolution at pH 4.5 is critical for stone wool, higher degradation was not observed in the case of WSW. Also, in terms of Si dissolution, virgin samples leach out more than waste samples.

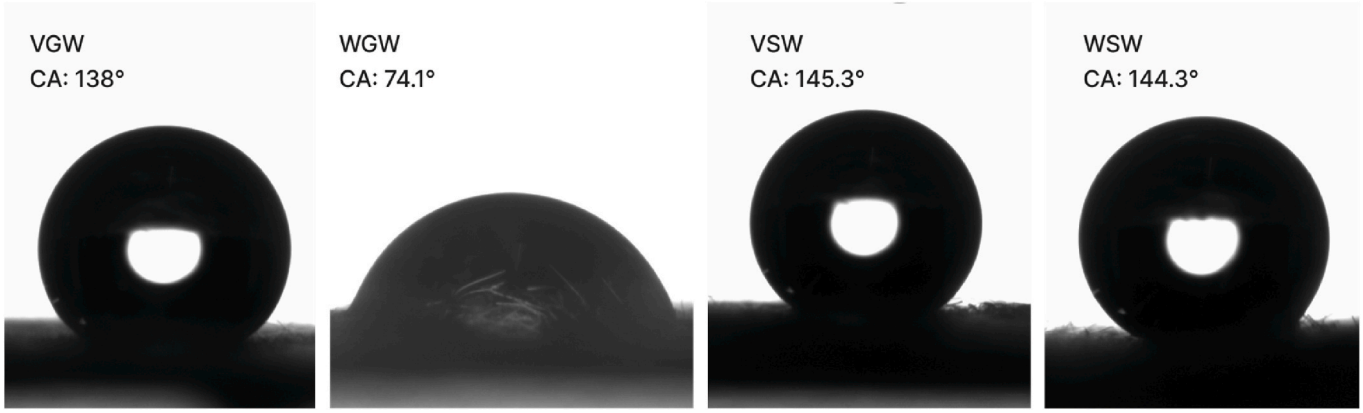

Fig. 5. Water contact angle of all the samples.

Table 5
Thermal conductivity of all mineral wool samples in different conditions.

Sample	Thermal conductivity, W/m·K			
	Loose state		Compressed state	
	Dry	Wet	Dry	Wet
VGW	0.0304 ± 0.000596	0.0756 ± 0.001330	0.0320 ± 0.000236	0.0914 ± 0.001918
WGW	0.0362 ± 0.000201	0.0689 ± 0.000064	0.0367 ± 0.000345	0.0974 ± 0.001375
VSW	0.0367 ± 0.000240	0.0498 ± 0.001180	0.0356 ± 0.000425	0.0421 ± 0.000775
WSW	0.0376 ± 0.000238	0.0525 ± 0.003442	0.0405 ± 0.000935	0.0580 ± 0.001271

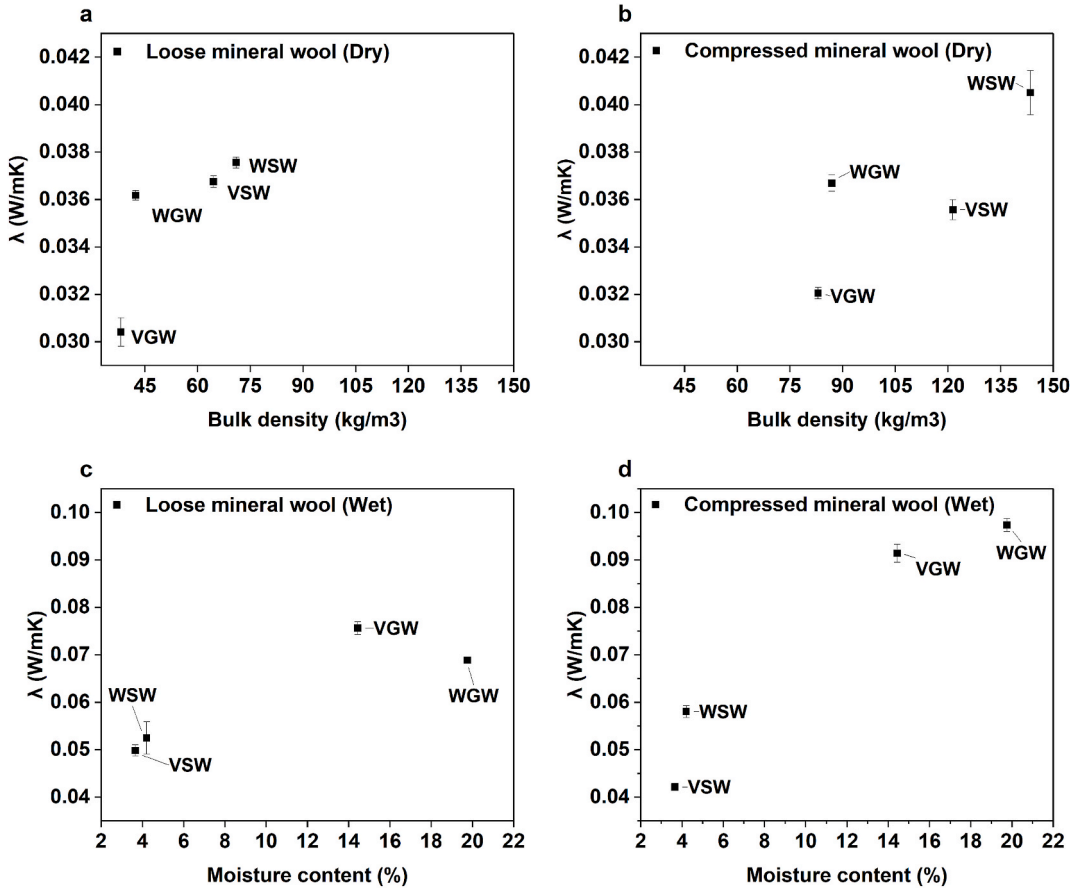

Fig. 6. Thermal conductivity; (a) Loose mineral wool (dry), (b) Compressed mineral wool (dry), (c) Loose mineral wool (wet), (d) Compressed mineral wool (wet).

Table 6
Summary of λ-values of WGW, WSW and available fibrous counterparts.

Type of material	Bulk density (kg/m3)	λ-value (W/m·K)	Reference
WGW	40 ≃ 70	0.0362	This study
WSW	40 ≃ 70	0.0376	
Bagasse	60 ≃ 100	0.034	Mehrzad et al. (2022)
Discarded face masks	60 ≃ 100	0.029	Dehdashti et al. (2024)
Polypropylene	60 ≃ 100	0.031	Karimi et al. (2022)
Sheep wool and hemp	60 ≃ 100	0.040	Pennacchio et al. (2017)
Jute	60 ≃ 100	0.038	Schiavoni et al. (2016)

3.3.2. Optical microscopy

The dimensional analysis of all the fibres was done by determining the aspect ratios of all the mineral wool samples. Table 7 indicates that the average aspect ratio of all the samples is greater than 3, which holds good with the standard prescribed by the World Health Organization (WHO, 1997). However, the minimum aspect ratio of WSW was less than 3 which indicates it to be carcinogenic (see Table 7).

Overall, the qualitative analysis (SEM) demonstrates that organic binder strongly influences the surface morphology and dissolution behaviour of mineral wool. On the other hand, quantitative analysis (optical microscopy) confirms that most fibers maintain aspect ratios within WHO standards, except WSW fibers that fall below this threshold. However, due to the low sample size (250 fibres), it is difficult to classify mineral wool as non-carcinogenic. Therefore, bio-solubility of such respirable fibers was determined using a dissolution rate and constant which is further explained in the following section.

3.4. Bio-solubility test

3.4.1. ICP-OES

The amounts of silicon (Si), aluminium (Al), calcium (Ca), and magnesium (Mg) in the effluent solution were quantified by ICP as shown in Fig. 9. Since silicon was the principal component of mineral wool, the amount of Si ions released was considered to be the key indicator of how long mineral wool persisted in synthetic lung fluid. Its release in Gamble solution was a valid parameter for the assessment of fiber behaviour throughout the dissolution process (Thelohan and De Meringo, 1994). It was observed that the Si dissolution was highest in VGW samples, and a significant dissolution was seen after 1 day until the 14th day. However, further dissolution was seen in the samples at a slower rate. A similar trend was observed with WGW until the 14th day, after which the dissolution of Si ions decreased linearly. In the case of stone wool samples (VSW and WSW), Si dissolution steadily occurred over different periods. The dissolution of Al started reducing for stone wool samples with increased periods. On the other hand, due to the lower aluminium content in the glass wool samples, they had negligible dissolution for aluminium.

Mg and Ca were considered as the leaching elements in the case of mineral wool; all the samples had an increased dissolution of these elements. Noticeably, calcium had the highest dissolution compared to magnesium due to its higher concentration in all the samples, which could be seen from the XRF results. However, a reduction in the dissolution of leaching elements was observed after 21 days in glass wool samples, and this was not observed in the stone wool. This could also be attributed to the differences in the chemical composition of the mineral wool samples, where higher Ca content was observed in stone wool samples compared to that of glass wool samples.

3.4.2. Dissolution rate (v) and dissolution constant (K_{dis})

The dissolution constant (K_{dis}) expressed in ng/cm^2/h, provides a metric about the fiber durability or in other words assesses the capacity of fibres to maintain integrity in simulated lung fluids (Cannizzaro et al., 2019). In addition, the dissolution rate (v) and K_{dis} of mineral wool samples are also influenced by the type of dissolution, (batch dissolution in this research compared to conventional continuous dissolution) different time periods, and the type of sample. The value of 'v' was calculated based on the weights of the mineral wool samples before and after the treatment (Thelohan and De Meringo, 1994).

The estimated dissolution constants (K_{dis}) for 14 and 28 days at pH 4.5 are shown in Table 8. K_{dis} was calculated for all fibres over a period of 14 days, in accordance with Guldberg et al. (1998), and treatments

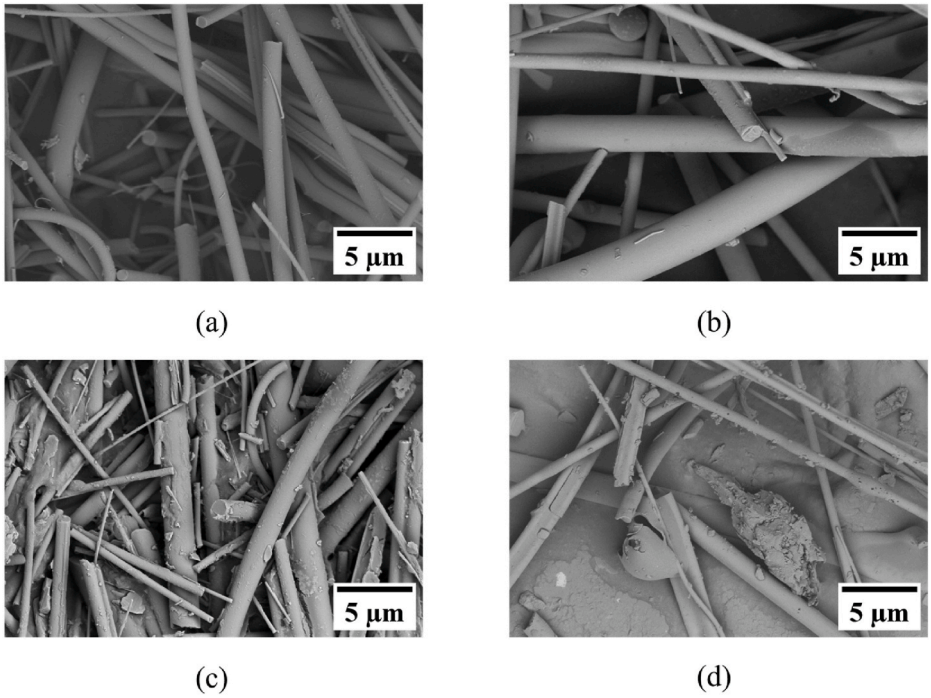

Fig. 7. SEM images of (a) VGW; (b) VSW; (c) WGW; (d) WSW before the bio-solubility test.

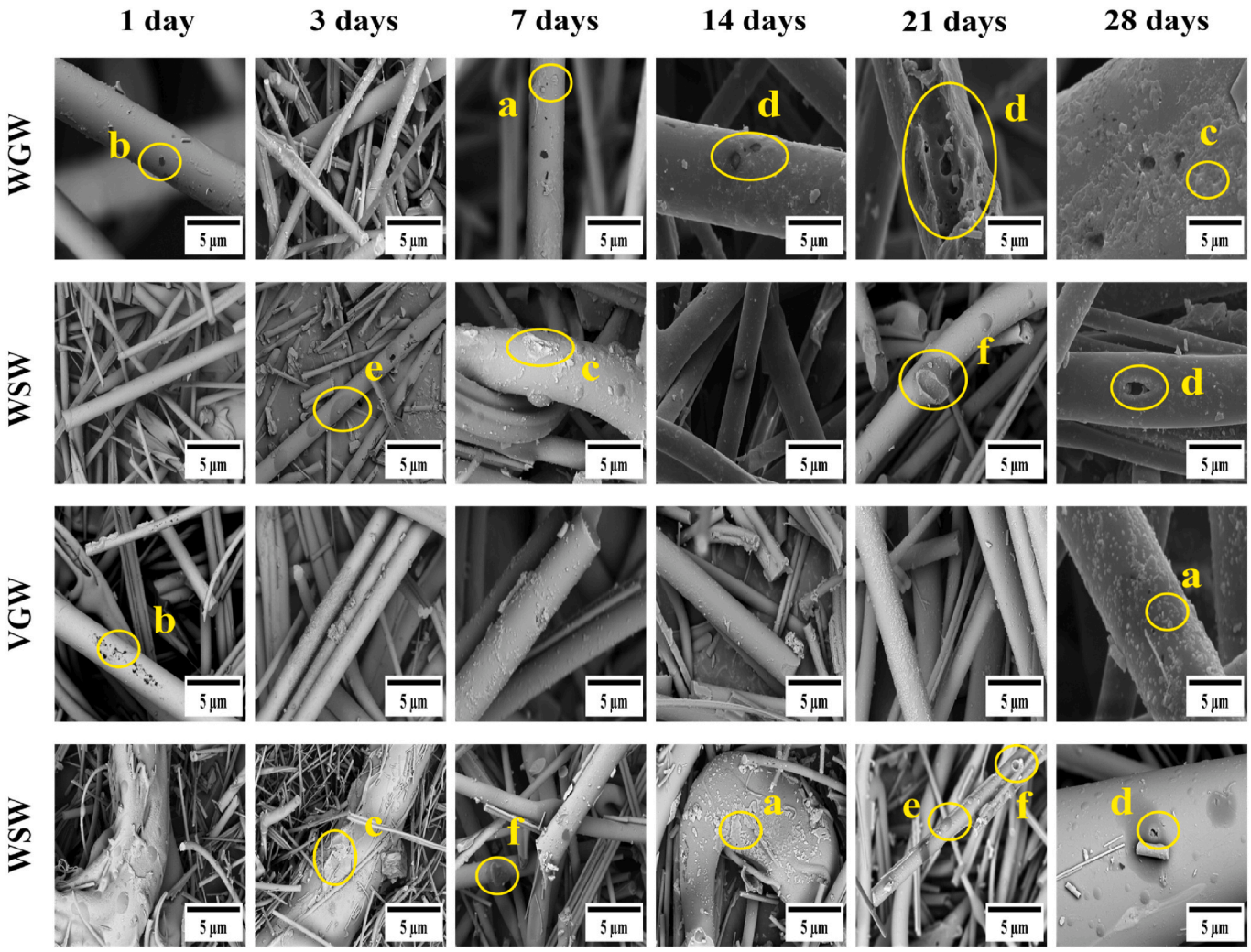

Fig. 8. SEM images of all the mineral wool samples after dissolution in MG solution at pH 4.5. Yellow circles indicate typical structural formation of (a) crystalline deposits, (b) layer removal, (c) characteristic gel formation, (d) leaching pits, (c) formation of bubbles, (f) collapse of bubbles.

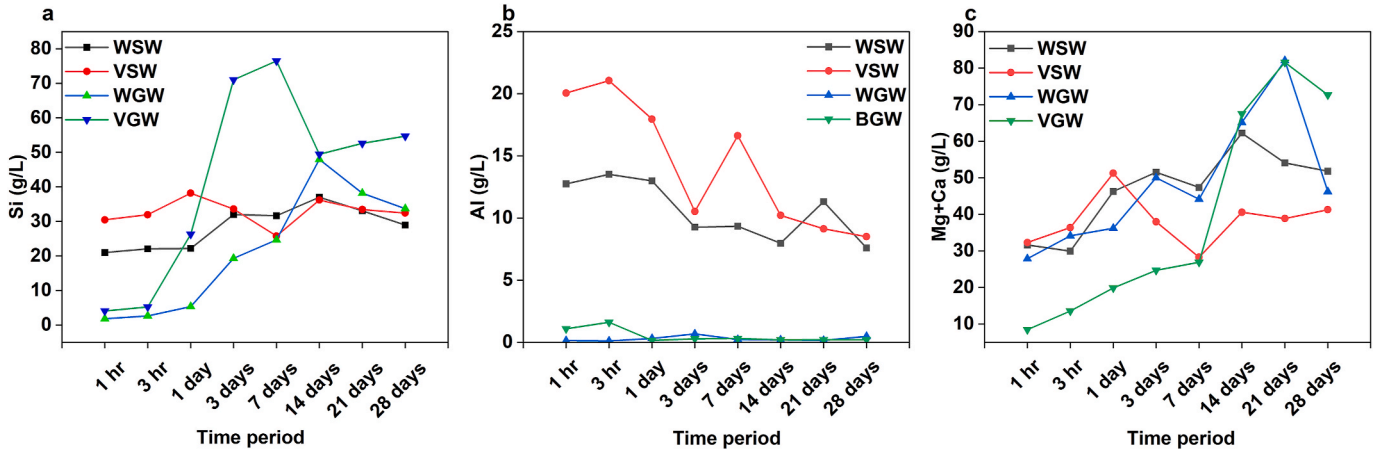

Fig. 9. Dissolution of elements for all mineral wool samples at pH 4.5; (a) Dissolution of Si; (b) Dissolution of Al; (c) Dissolution of leaching elements (Mg + Ca).

lasting 14 and 28 days were chosen for comparison. After 14 days, glass wool samples—which dissolve easily at pH 7.5 (Christensen et al., 1994; Guldberg et al., 1998), which is almost neutral—displayed less dissolution than VSW. Supersaturation caused by high Si and leaching element release in VGW (Fig. 9) limited additional dissolution by 28 days. At 14 days, the K_{dis} of the two glass wool samples were comparable; however, at 28 days, WGW's K_{dis} was more than twice that of VGW. The observed dissolution behaviour was consistent with Si-gel formation mechanisms reported in the literature, which influence fiber degradation rates (Wohlleben et al., 2017; Sauer et al., 2021).

Table 7
Aspect ratio of all the samples.

Sample	Minimum aspect ratio	Mean aspect ratio
VGW	3.27	26.60 ± 24.58
VSW	3.26	23.30 ± 15.76
WGW	4.06	31.22 ± 32.13
WSW	2.14	26.69 ± 23.58

Table 8
Dissolution constant after 14 and 28 days.

Samples	Dissolution constant K_{dis} (ng/cm^2/h)	
	14 days	**28 days**
VGW	108.42	18.99
WGW	105.97	51.49
VSW	454.66	19.23
WSW	79.17	3.14

On the other hand, stone wool samples – soluble at pH 4.5 – such as VSW had K_{dis} 4–5 times higher than WSW at 14 days and 6 times higher at 28 days. WSW did not surpass the 400 ng/cm^2/h exoneration threshold recommended by Guldberg et al. (2002). However, prior research (Eastes and Hadiey, 1995; Eastes and Hadley, 1996) on animals demonstrated that fibres with K_{dis} >100 ng/cm^2/h did not cause tumors or fibrosis, suggesting that VGW and WGW after 14 days would be regarded as safe in terms of their effects on the respiratory system.

The dissolution behavior exhibited in this study corresponds to results obtained under a static *in-vitro* technique at pH 4.5, thus being specific to the selected test conditions, and the specific set of waste and virgin samples analyzed. Although variations in dissolution rates indicate relative bio-persistence, such data should not be interpreted as direct evidence of toxicity or safety, as *in-vitro* dissolution does not replicate the complexities of respiratory exposure pathways, clearance mechanisms, or *in-vivo* physiological conditions. Therefore, the data should be regarded as comparing trends rather than indicators of health outcomes. Nonetheless, waste mineral wool, which does not surpass biosolubility can be upcycled into new building materials such as aerogels, avoiding landfills.

4. Conclusion

In the effort to tackle environmental problems associated with waste mineral wool such as landfilling or incineration. This work focuses on the waste mineral wool characterization, in order to study the feasibility of reusing it for blown-in insulation applications. Moreover, the corresponding risks associated with the use of short-fibrous materials was also addressed. An assessment of various properties of waste mineral wool revealed that after 30 years of service life, it retained the potential properties required for insulation applications. The following conclusions can be drawn from this study:

- XRF and FTIR analyses demonstrated that waste mineral wool maintained chemical compositions similar to those of virgin materials, suggesting that prolonged service exposure does not substantially modify the primary oxide structure of the fibres.
- Ageing causes the deterioration of organic binders, leading to increased moisture sensitivity, with water absorption increasing by around 33% (WGW) and 101% (WSW). This trend was consistently observed in vapour sorption and contact angle measurements.
- Thermal conductivity increased in dry WGW by 19% (loose) and 15% (compressed) compared to VGW under similar conditions. Similarly, an increasing trend of 2% in dry WSW (loose) and 14% in WSW (compressed) was observed.
- Waste mineral wool samples had λ-values within the permitted range (0.03-0.04 W/m·K), and are similar to natural and non-traditional insulating materials. This recommends their usage in blown-in insulation, cavity walls, and prefabricated facade and roof components, meeting the EU's 70% building and demolition waste recovery goal.
- SEM analysis revealed surface dissolution features such as leaching pits, layer removal and silica-rich gel formation after exposure to simulated lung fluid, indicating ongoing fiber degradation under physiological conditions.
- Bio-solubility tests showed that K_{dis} for VGW, VSW and WGW during *in-vitro* method at pH 4.5 reaches the threshold level after 14 days, unlike WSW, which does not reach the minimum threshold of 100 ng/cm^2/h. The presented results are best interpreted as categorizing tool of different fibers rather than health-risk indicators. The extrapolation of these findings to human health risk is not feasible without further investigation, as fiber pathogenicity is affected by multiple factors, including number of replicates, exposure levels, respirable fiber fractions, bio-durability under physiological pH conditions, and *in-vivo* clearance pathways.

CRediT authorship contribution statement

S. Tumkur Karnick: Conceptualization, Data curation, Investigation, Methodology, Visualization, Writing – original draft, Writing – review & editing. **N. Lushnikova:** Methodology, Supervision, Writing – original draft, Writing – review & editing. **F. Gauvin:** Supervision, Writing – review & editing. **H.J.H. Brouwers:** Supervision, Writing – review & editing.

Declaration of competing interest

The authors declare that they have no known competing financial interests or personal relationships that could have appeared to influence the work reported in this paper.

Acknowledgement

The authors would like to acknowledge the financial support provided by Takkenkamp Groep, Kruiswijk, and M2i (Materials Innovation Institute), under the project entitled T22018 – "Improving circularity of mineral wool". Additionally, the authors would like to acknowledge Anneke Delsing for her assistance with the ICP-OES measurement.

Data availability

Data will be made available on request.

References

A New Circular Economy Action Plan - for a cleaner and more competitive Europe | Circular Cities and Regions Initiative. Off. J. Eur. Union, 2024. https://circular-cities-and-regions.ec.europa.eu/support-materials/eu-regulations-legislation/new-circular-economy-action-plan-cleaner-and-more. (Accessed 23 March 2026).

Abu-Jdayil, B., Mourad, A.H., Hittini, W., Hassan, M., Hameedi, S., 2019. Traditional, state-of-the-art and renewable thermal building insulation materials: an overview. Constr. Build. Mater. 214, 709–735. https://doi.org/10.1016/J.CONBUILDMAT.2019.04.102.

Acar, G., Steeman, M., Van Den Bossche, N., 2024. Reusing thermal insulation materials: reuse potential and durability assessment of stone wool insulation in flat roofs. Sustainability (Switzerland) 16. https://doi.org/10.3390/su16041657.

Agency for Toxic Substances and Disease Registry (US), 2004. Toxicological Profile for Synthetic Vitreous Fibers. National Library of Medicine, pp. 163–170. https://www.ncbi.nlm.nih.gov/books/NBK600969/. (Accessed 24 March 2026).

Asemani, M., Rabbani, A.R., 2020. Detailed FTIR spectroscopy characterization of crude oil extracted asphaltenes: curve resolve of overlapping bands. J. Pet. Sci. Eng. 185, 106618. https://doi.org/10.1016/J.PETROL.2019.106618.

Barly, S.H.Q., Okhrimenko, D.V., Solvang, M., Yue, Y., Stipp, S.L.S., 2019. Dissolution of stone wool fibers with phenol-urea-formaldehyde binder in a synthetic lung fluid. Chem. Res. Toxicol. 32, 2398–2410. https://doi.org/10.1021/acs.chemrestox.9b00179.

Borzova, M., Gauvin, F., Schollbach, K., 2025. Upcycling waste mineral wool into ambient pressure-dried silica aerogels. ACS Sustain. Chem. Eng. https://doi.org/10.1021/acssuschemeng.4c09976.
Cannizzaro, A., Angelosanto, F., Barrese, E., Campopiano, A., 2019. Biosolubility of high temperature insulation wools in simulated lung fluids. J. Occup. Med. Toxicol. 14. https://doi.org/10.1186/s12995-019-0235-z.
Christensen, V.R., Lund Jensen, S., Guldberg, M., 1994. Effect of chemical composition of man-made vitreous fibers on the rate of dissolution in vitro at different pHs. Environ. Health Perspect. 102, 83–86. https://doi.org/10.1289/ehp.94102s583.
Consultants, I.A.L., 2023. The European Market for Thermal Insulation Products. www.ialconsultants.com.
Coury, C., Dillner, A.M., 2008. A method to quantify organic functional groups and inorganic compounds in ambient aerosols using attenuated total reflectance FTIR spectroscopy and multivariate chemometric techniques. Atmos. Environ. 42, 5923–5932. https://doi.org/10.1016/J.ATMOSENV.2008.03.026.
Criado, M., Sobrados, I., Sanz, J., 2014. Polymerization of hybrid organic–inorganic materials from several silicon compounds followed by TGA/DTA, FTIR and NMR techniques. Prog. Org. Coating 77, 880–891. https://doi.org/10.1016/J.PORGCOAT.2014.01.019.
Dastorian Jamnani, B., Hosseini, S., Shavandi, A., Hassan, M.R., 2016. Thermochemical properties of Glass Wool/Maerogel composites. Adv. Mater. Sci. Eng. 2016. https://doi.org/10.1155/2016/6014874.
Dehdashti, Z., Soltani, P., Taban, E., 2024. Utilizing discarded face masks to fabricate sustainable high-performance panels for enhanced building thermal and acoustic comfort. J. Clean. Prod. 446, 141304. https://doi.org/10.1016/j.jclepro.2024.141304.
Directive (EU), 2024. 2024/1275 - energy performance of buildings directive. Off. J. Eur. Union. https://energy.ec.europa.eu/topics/energy-efficiency/energy-performance-buildings/energy-performance-buildings-directive_en. (Accessed 19 March 2026).
Doggett, M.S., 2020. Mineral Wool and Polyisocyanurate Insulation: a Comparative Study of Water Absorption, Drying and Rewetting.
Domonkos, M., Zobal, O., Prošek, Z., Trejbal, J., 2022. Thermal properties of mineral wool insulation recovered from construction and demolition waste. In: Acta Polytech. CTU Proc., Czech Technical University in Prague, pp. 6–10. https://doi.org/10.14311/APP.2022.34.0006.
Doschek-Held, K., Krammer, A.C., Steindl, F.R., Sattler, T., Juhart, J., 2024. Recycling of mineral wool waste as supplementary cementitious material through thermochemical treatment. Waste Manage. Res. https://doi.org/10.1177/0734242X241237199.
Eastes, Walter, Hadiey, John G., 1995. Dissolution of fibers inhaled by rats. Inhal. Toxicol. 7, 179–196.
Eastes, Walter, Hadley, John G., 1996. A mathematical model of fiber carcinogenicity and fibrosis in inhalation and intraperitoneal experiments in rats. Inhal. Toxicol. 8, 323–343.
EURIMA, How is Mineral Wool Insulation Made, (n.d.). https://www.eurima.org/how-is-mineral-wool-insulationmade (accessed March 18, 2025).
EURIMA, European Parliament and Council, 2008. Regulation (EC) No 1272/2008 of the European Parliament and of the Council of 16 December 2008 on Classification, Labelling and Packaging of Substances and Mixtures, Amending and Repealing Directives 67/548/EEC and 1999/45/EC, and Amending Regulation (EC) No 1907/2006. Strabourg, 2008.
Glass Wool: Applications and Thermal Conductivity, (n.d.). https://www.huameiworld.com/news/glass-wool-applications-and-thermal-conductivity.html (accessed May 8, 2025).
Guldberg, M., Christensen, V.R., Perander, M., Zoitos, B., Koenig, A.R., Sebastian, K., 1998. Measurement of In-Vitro fibre dissolution rate at acidic pH. Pergamon Ann. Orcup. Hyg. 42, 233–243.
Guldberg, M., De Meringo, A., Kamstrup, O., Furtak, H., Rossiter, C., 2000. The development of glass and stone wool compositions with increased biosolubility. Regul. Toxicol. Pharmacol. 32, 184–189. https://doi.org/10.1006/rtph.2000.1418.
Guldberg, M., Jensen, S.L., Knudsen, T., Steenberg, T., Kamstrup, O., 2002. High-alumina low-silica HT stone wool fibers: a chemical compositional range with high biosolubility. Regul. Toxicol. Pharmacol. 35, 217–226. https://doi.org/10.1006/rtph.2001.1523.
Hasanzadeh, R., Azdast, T., Lee, P.C., Park, C.B., 2023. A review of the state-of-the-art on thermal insulation performance of polymeric foams. Therm. Sci. Eng. Prog. 41. https://doi.org/10.1016/j.tsep.2023.101808.
Health Effects Institute-Asbestos Research, 1991. Asbestos in Public and Commercial Buildings: a Literature Review and Synthesis of Current Knowledge.
Jiřičková, M., Pavlík, Z., Fiala, L., Černý, R., 2006. Thermal conductivity of mineral wool materials partially saturated by water. Int. J. Thermophys. 27, 1214–1227. https://doi.org/10.1007/s10765-006-0076-8.
Karimi, F., Soltani, P., Zarrebini, M., Hassanpour, A., 2022. Acoustic and thermal performance of polypropylene nonwoven fabrics for insulation in buildings. J. Build. Eng. 50, 104125. https://doi.org/10.1016/j.jobe.2022.104125.
Kläusler, O., Clauß, S., Lübke, L., Trachsel, J., Niemz, P., 2013. Influence of moisture on stress–strain behaviour of adhesives used for structural bonding of wood. Int. J. Adhesion Adhes. 44, 57–65. https://doi.org/10.1016/J.IJADHADH.2013.01.015.
Koh, C.H., Luo, Y., Schollbach, K., Gauvin, F., Brouwers, H.J.H., 2024. A circular approach to stone wool: Alkali-activated lightweight aggregates. Developments in the Built Environment 19. https://doi.org/10.1016/j.dibe.2024.100506.
Komkova, A., Agergaard, S.K., Holt Andersen, B., Habert, G., 2025. Identifying barriers and enablers for emerging value chains in open-loop mineral wool waste recycling within the construction sector. Dev. Built Environ. 22, 100662. https://doi.org/10.1016/J.DIBE.2025.100662.
Level(s) - construction products Europe, (n.d.). https://construction-products.eu/publications/levels/(accessed March 23, 2026).
Lin, S., Liu, Z., Zhao, E., Qian, J., Li, X., Zhang, Q., Ali, M., 2019. A study on the FTIR spectra of pre- and post-explosion coal dust to evaluate the effect of functional groups on dust explosion. Process Saf. Environ. Prot. 130, 48–56. https://doi.org/10.1016/J.PSEP.2019.07.018.
Martin, J.W., 2006. In: 4 - Glasses and Ceramics, Third. Woodhead Publishing. https://doi.org/10.1533/9781845691608.2.133.
Mehrzad, S., Taban, E., Soltani, P., Samaei, S.E., Khavanin, A., 2022. Sugarcane bagasse waste fibers as novel thermal insulation and sound-absorbing materials for application in sustainable buildings. Build. Environ. 211, 108753. https://doi.org/10.1016/j.buildenv.2022.108753.
Mineral Wool Insulation Material Market Size, Share & Analysis 2033 Report, 2024. https://www.globalgrowthinsights.com/market-reports/mineral-wool-insulation-material-market-108040. (Accessed 31 March 2025).
Nilsen, E., Puputti, J., Lindén, M., Le Bell, J., Perander, M., Einarsrud, M.A., 2003. Sol-gel derived binder for inorganic composites. J. Sol. Gel Sci. Technol. 26, 1239–1242. https://doi.org/10.1023/A:1020780823598/METRICS.
Pavlin, M., Horvat, B., Frankovič, A., Ducman, V., 2021. Mechanical, microstructural and mineralogical evaluation of alkali-activated waste glass and stone wool. Ceram. Int. 47, 15102–15113. https://doi.org/10.1016/j.ceramint.2021.02.068.
Pennacchio, R., Savio, L., Bosia, D., Thiebat, F., Piccablotto, G., Patrucco, A., Fantucci, S., 2017. Fitness: Sheep-wool and hemp sustainable insulation panels. Energy Proc. 111, 287–297. https://doi.org/10.1016/j.egypro.2017.03.030.
Rahla, K.M., Mateus, R., Bragança, L., 2021. Implementing Circular economy strategies in Buildings—From theory to practice. Appl.Syst. Innov. 4. https://doi.org/10.3390/ASI4020026, 26 4 (2021) 26.
Ramsey, M.H., Potts, P.J., Webb, P.C., Watkins, P., Watson, J.S., Coles, B.J., 1995. An objective assessment of analytical method precision: comparison of ICP-AES and XRF for the analysis of silicate rocks. Chem. Geol. 124, 1–19. https://doi.org/10.1016/0009-2541(95)00020-M.
Regulation - EU - 2024/3110 - EN - EUR-Lex, 2024. Off. J. Eur. Union. https://eur-lex.europa.eu/eli/reg/2024/3110/oj/eng. (Accessed 23 March 2026).
Regulation (EU) 2024/1781 - EN - EUR-Lex, 2024. Off. J. Eur. Union. https://eur-lex.europa.eu/eli/reg/2024/1781/oj/eng. (Accessed 23 March 2026).
Rengasamy, R.S., 2006. Wetting phenomena in fibrous materials, Thermal and Moisture Transport in Fibrous materials. https://doi.org/10.1533/9781845692261.1.156.
Rywotycki, M., Cebo-Rudnicka, A., Szajding, A., Kąc, S., Rikardsen, M., Heggelund, J., Tretel, P., Jerzak, W., 2024. Thermal removal of binder from waste glass wool intended for recycling. J. Therm. Anal. Calorim. https://doi.org/10.1007/s10973-024-13661-z.
Sattler, T., Pomberger, R., Schimek, J., Vollprecht, D., 2020. Mineral wool waste in Austria, associated health aspects and recycling options. Detritus 9, 174–180. https://doi.org/10.31025/2611-4135/2020.13904.
Sauer, U.G., Werle, K., Waindok, H., Hirth, S., Hachmöller, O., Wohlleben, W., 2021. Critical choices in predicting stone wool biodurability: lysosomal fluid compositions and binder effects. Chem. Res. Toxicol. 34, 780–792. https://doi.org/10.1021/acs.chemrestox.0c00401.
Schiavoni, S., D'Alessandro, F., Bianchi, F., Asdrubali, F., 2016. Insulation materials for the building sector: a review and comparative analysis. Renew. Sustain. Energy Rev. 62, 988–1011. https://doi.org/10.1016/j.rser.2016.05.045.
Snellings, R., 2013. Solution-Controlled dissolution of supplementary cementitious material glasses at pH 13: the effect of solution composition on glass dissolution rates. J. Am. Ceram. Soc. 96, 2467–2475. https://doi.org/10.1111/JACE.12480.
Straub, A., van Nunen, H., Janssen, R., Maam, L., 2011. Levensduur Van Bouwproducten. Methode Voor Referentiewaarden. SBR.
Superti, V., Forman, T.V., Houmani, C., 2021. Recycling thermal insulation materials: a case Study on more circular management of expanded polystyrene and stonewool in Switzerland and research agenda. Resources 10. https://doi.org/10.3390/RESOURCES10100104, 104 10 (2021) 104.
Thelohan, S., De Meringo, A., 1994. In vitro dynamic solubility Test: influence of various pararmeters. Environ. Health Perspect. 102, 91–96.
Väntsi, O., Kärki, T., 2014. Mineral wool waste in Europe: a review of mineral wool waste quantity, quality, and current recycling methods. J. Mater. Cycles Waste Manag. 16, 62–72. https://doi.org/10.1007/s10163-013-0170-5.
WHO, 1997. Determination of Airborne Fiber Number Concentrations: a Recommended Method, by Phase Contrast Optical Microscopy (Membrane Filter Method).
Wohlleben, W., Waindok, H., Daumann, B., Werle, K., Drum, M., Egenolf, H., 2017. Composition, respirable fraction and dissolution rate of 24 stone wool MMVF with their binder. Part. Fibre Toxicol. 14. https://doi.org/10.1186/s12989-017-0210-8.
Yap, Z.S., Khalid, N.H.A., Haron, Z., Mohamed, A., Tahir, M.M., Hasyim, S., Saggaff, A., 2021. Waste mineral wool and its opportunities—a review. Materials 14. https://doi.org/10.3390/ma14195777.
Yliniemi, J., Laitinen, O., Kinnunen, P., Illikainen, M., 2018. Pulverization of fibrous mineral wool waste. J. Mater. Cycles Waste Manag. 20, 1248–1256. https://doi.org/10.1007/s10163-017-0692-3.
Yliniemi, J., Ramaswamy, R., Luukkonen, T., Laitinen, O., de Sousa, Á.N., Huuhtanen, M., Illikainen, M., 2021. Characterization of mineral wool waste chemical composition, organic resin content and fiber dimensions: aspects for valorization. Waste Manag. 131, 323–330. https://doi.org/10.1016/j.wasman.2021.06.022.

Yu, Y., Xu, P., Chang, M., Chang, J., 2018. Aging properties of phenol-formaldehyde resin modified by bio-oil using UV weathering. Polymers (Basel) 10. https://doi.org/10.3390/polym10111183.

Zhong, Y., Jiang, Q., Qi, T., Lu, H., Wei, S., Cui, P., Yang, W., Hao, W., 2025b. Sustainable development: High-value conversion of waste mineral wool into magnetic oil absorbents. J. Environ. Chem. Eng. 13, 117080. https://doi.org/10.1016/J.JECE.2025.117080.

Zhong, Y., Pan, X., Qi, T., Lu, H., Wei, S., Cui, P., Yang, W., Hao, W., 2025a. Converting waste mineral wool to value-added multifunctional composites in a single step. Sustain. Mater. Technol. 45, e01480. https://doi.org/10.1016/J.SUSMAT.2025.E01480.